











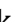

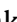















# Accurate simultaneous lead stopping power and charge-state measurements in gases and solids: Benchmark data for basic atomic theory and nuclear applications

S. Ishikawa<sup>a, , 1</sup>, H. Geissel<sup>b, c, </sup>, S. Purushothaman<sup>b, , \*</sup>, H. Weick<sup>b, </sup>, E. Haettner<sup>b, </sup>, N. Iwasa<sup>a, </sup>, C. Scheidenberger<sup>b, c, d, </sup>, A.H. Sørensen<sup>e</sup>, Y.K. Tanaka<sup>f, </sup>, T. Abel<sup>g</sup>, J. Äystö<sup>h, i, </sup>, S. Bagchi<sup>j, </sup>, T. Dickel<sup>b, c, </sup>, V. Drozd<sup>k, b, </sup>, B. Franczak<sup>b, </sup>, F. Greiner<sup>b, </sup>, M.N. Harakeh<sup>k, </sup>, N. Kalantar-Nayestanaki<sup>k, </sup>, B. Kindler<sup>b, </sup>, R. Knöbel<sup>b, </sup>, D. Kostyleva<sup>b, </sup>, S. Kraft-Bermuth<sup>l, </sup>, N. Kuzminchuk<sup>b, </sup>, E. Lamour<sup>m, </sup>, B. Lommel<sup>b, </sup>, I. Mukha<sup>b, </sup>, Z. Patyk<sup>n, </sup>, S. Pietri<sup>b, </sup>, G. Schaumann<sup>g, </sup>, J. Zhao<sup>b, </sup> for the Super-FRS Experiment Collaboration

<sup>a</sup> Department of Physics, Tohoku University, Sendai, 980-8578, Japan

<sup>b</sup> GSI Helmholtzzentrum für Heavy Ion Research, Darmstadt, 64291, Germany

<sup>c</sup> II. Physics Institute, Justus Liebig University, Gießen, 35392, Germany

<sup>d</sup> Helmholtz Research Academy Hesse for FAIR (HFHF), GSI Helmholtz Center for Heavy Ion Research, Campus Gießen, Gießen, 35392, Germany

<sup>e</sup> Department of Physics and Astronomy, Aarhus University, Aarhus C, 8000, Denmark

<sup>f</sup> RIKEN Cluster for Pioneering Research, RIKEN, Saitama, 351-0198, Japan

<sup>g</sup> Institut für Kernphysik, Technischen Universität Darmstadt, Darmstadt, 64289, Germany

<sup>h</sup> Helsinki Institute of Physics, Helsinki, 00560, Finland

<sup>i</sup> Department of Physics, University of Jyväskylä, Jyväskylä, 40500, Finland

<sup>j</sup> Indian Institute of Technology (ISM) Dhanbad, Dhanbad, 826004, Jharkhand, India

<sup>k</sup> ESRIG, University of Groningen, AG Groningen, 9747, the Netherlands

<sup>l</sup> Institute for Medical Physics and Radiation Protection, Technische Hochschule Mittelhessen, Gießen, 35390, Germany

<sup>m</sup> Institut des Nanosciences de Paris, Sorbonne Université, CNRS UMR 7588, Paris, 75005, France

<sup>n</sup> Nuclear Physics Division, National Centre for Nuclear Research, Warszawa, 02-093, Poland

## ARTICLE INFO

### Article history:

Received 9 June 2023

Received in revised form 6 September 2023

Accepted 27 September 2023

Available online 4 October 2023

Editor: D.F. Geesaman

### Keywords:

Heavy ion

Stopping power

Mean charge state

Bohr-Lindhard density effect

## ABSTRACT

We have measured for the first time simultaneously both the mean charge states and stopping powers of (35–280) MeV/u <sup>208</sup>Pb ions in gases and solids with an accuracy of 1%. The existence at lower energies and disappearance at higher of density effects in the charge-state distribution and the corresponding stopping power are directly confirmed and comparisons with widely used theories and simulations for heavy ions demonstrate strong deviations of up to 27%. However, an unprecedented prediction power of better than 3% has been achieved for the energy loss when the measured mean charge-states are implemented in the Lindhard-Sørensen theory. Our present benchmark data contribute to an improved understanding of the basic atomic collision processes and to numerous applications in nuclear physics. Extending the GANIL data [1] to higher accuracy and energies, we can now answer at which velocities the Bohr-Lindhard density effect in stopping will vanish.

© 2023 The Authors. Published by Elsevier B.V. This is an open access article under the CC BY license (<http://creativecommons.org/licenses/by/4.0/>). Funded by SCOAP<sup>3</sup>.

When fast ions penetrate through matter, they primarily lose their kinetic energy due to elastic and inelastic collisions with the atoms of the material traversed [2,3]. In addition, the ions change their direction and may even change the ionic charge states, depending on the velocity and element number. Charge-changing collisions and the resulting charge-state distribution are character-

\* Corresponding author.

E-mail address: [S.Purushothaman@gsi.de](mailto:S.Purushothaman@gsi.de) (S. Purushothaman).

<sup>1</sup> Part of doctoral thesis.

istics of heavy ions and are important over a large velocity range, contrary to protons or alpha particles, i.e., they affect the energy loss.

The application of stopping power spans various scientific disciplines, including ion implantation, radiation therapy, materials science, nuclear physics, and rare isotope production. The results of the present experiment have particular relevance for investigating  $N=126$  nuclei, which are important in astrophysics [4] and can be produced and spatially separated in-flight using a primary lead beam. The isotopic separation of rare isotopes in flight is based on precise energy-loss measurements in thick degraders placed at dispersive focal planes of fragment separators. The latter separation method is worldwide used in nearly all large-scale nuclear beam facilities, e.g. [5,6]. Additionally, accurate knowledge of stopping power is essential for tumor irradiation near sensitive organs [7,8], implantation of rare isotopes in solids and gases [9–11], and particle identification through energy deposition in ionization chambers. In these applications, precise knowledge is required within the few-percentage domain or even better.

Fission fragments were the first heavy ions studied [12]. N. O. Lassen discovered experimentally that the mean charge state of fission fragments was higher when they emerged from solids compared to gases at the same velocity. N. Bohr and J. Lindhard [13] explained this experimental observation by the higher collision frequency in solids, leading to projectiles excited in successive collisions, whereas the projectiles in a dilute gaseous medium return to the ground state between collisions. To honor these pioneers, we name the gas-solid differences caused by ionization of the projectile inside the target as the “Lassen density effect” for charge states and the “Bohr-Lindhard density effect” for stopping powers.

Betz and Grodzins [14] postulated a model in which the difference in the observed mean charge states occurs when the excited ions emerge from the solids and de-excite via Auger-electron emission. The experimental observation and the conflicting interpretation were, for a long period, not solved.

Important improvements were only possible with the advent of heavy-ion accelerators, which could provide monoenergetic projectiles with a small emittance. However, this technical progress of the first-generation heavy-ion accelerators was not sufficient because the maximum energy was not high enough, and thus the so-called  $Z_2$ -oscillation [15] obscured the observation of a gas-solid difference of neighboring elements. In atomic-collision publications,  $Z_1$  and  $Z_2$  are the element numbers of the projectile and target, respectively.

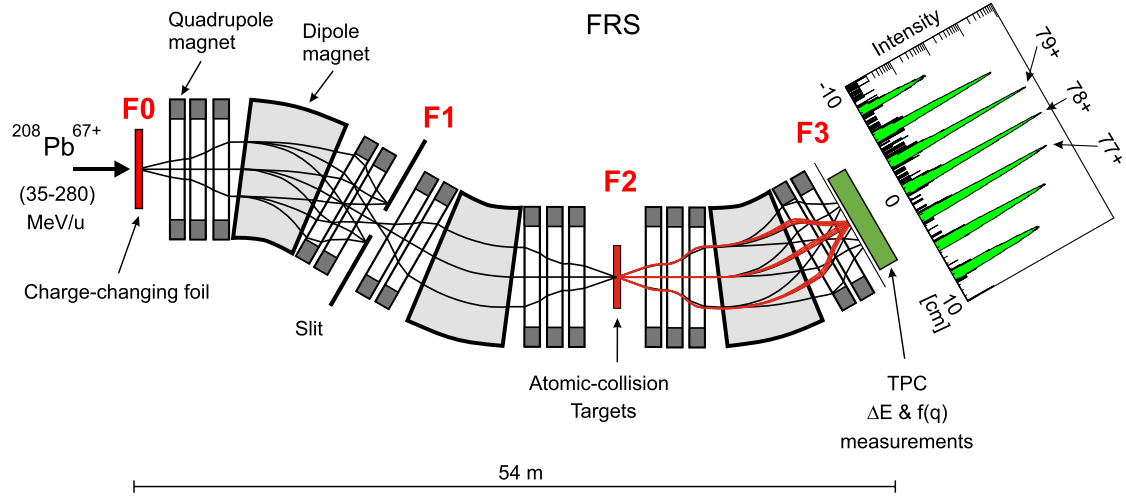
Furthermore, the predicted number of Auger-electrons has not been found despite great experimental efforts over several decades [16]. An indirect experimental signature of an increased charge state inside solids was the increased production of inner-shell vacancies observed in x-ray emission. A substantial experimental improvement to solve this puzzle was realized with the universal heavy-ion accelerator UNILAC at GSI, which could not only deliver projectiles of all elements up to uranium but also high energies to bypass the structural electronic target effects, the  $Z_2$ -oscillation. With this experimental progress, the Bohr-Lindhard density effect was for the first time clearly observed in systematic stopping-power measurements [17,18]. Independent gas-solid stopping-power measurements were also performed at the powerful INPO and GANIL accelerator facilities in France a few years later [19]. Those experiments confirmed the gas-solid difference in stopping powers discovered at GSI. The important remaining question was, at which velocity the effect will vanish. The GANIL experiments with lead and uranium projectiles were at much lower velocities and do not enter the energy domain where the gas-solid difference will vanish. Furthermore, they have the disadvantage that the results for solids are not directly measured but obtained via an empirical effective-charge scaling [1].

Despite the experimental observation of the Bohr-Lindhard density effect, it has not been included in the widely-used theoretical descriptions and simulations due to the complexity of charge-changing collisions and strong deviation from descriptions based on first Born approximation (Bethe theory). Motivated by this situation, we have performed the first simultaneous measurements of charge-state distributions and stopping powers for (35–280) MeV/u  $^{208}\text{Pb}$  projectiles in gases and solids at many energies. The energy range was selected such that the Bohr-Lindhard effect should be observed at lower velocities and should have vanished by 280 MeV/u. Furthermore, we aimed at precise stopping-power predictions using the simultaneously measured charge-state distribution. These basic investigations are worldwide unique and thus extend the knowledge and applications of atomic ion-matter interaction.

The experimental goals were achieved with the versatile and flexible UNILAC and synchrotron SIS-18 accelerator systems [20], in combination with the fragment separator FRS [21]. The FRS was used as a multiple-stage, high-resolution magnetic spectrometer to determine the energy loss and charge-state distribution. FRS, with its versatile ion-optical system and the particle detectors at the focal planes, is ideally suited for atomic-collision experiments as demonstrated in previous experiments [9,22–25]. The charge-state  $67^+$  of the accelerated  $^{208}\text{Pb}$  beam extracted from the synchrotron SIS-18 is fixed for all energies because it is determined by the stripping section in the synchrotron injection channel. The projectiles from SIS-18 are transported via a magnetic beam line to the entrance of the FRS. Here, they interact with a charge-changing foil, see Fig. 1. An appropriate incident charge state for the measurement is selected at the first dispersive focal plane F1 before the ions impinge on the atomic-collision targets at F2. These targets can be either solid foils or a gaseous medium confined within window-sealed gas cells.

The thicknesses of the different solid and gaseous targets were selected to cause approximately (5–30)% energy loss. The first goal was to select the incident charge state very close to the mean charge determined by the targets for each energy provided by SIS-18. The influence of the solid windows of the gas targets was taken care of by separate measurements using a single target of the same material and thickness as was used for the gas-cell windows. The energy loss and the charge-state distribution were measured for each target with a position-sensitive time-projection chamber (TPC) at the dispersive focal plane F3. The position resolution of this detector was  $\pm 0.1$  mm. An essential part of these measurements was the determination of the absolute magnetic rigidity value without and with the targets inserted.

The incident energy is known from the synchrotron calibration with an accuracy of approximately  $5 \times 10^{-4}$ . This calibration is based on frequency and position measurements of the circulating beam inside SIS-18 before it is extracted. The energy loss in different charge-changing foils of a known thickness ( $2\text{--}14 \mu\text{g}/\text{cm}^2$ ) causes a minor correction for the incident energy. The  $^{208}\text{Pb}$  ions, with a selected charge state, were first centered at both focal planes, F2 and F3, without a target inserted. With the calibrated SIS energy, the known mass and charge state, and the calibrated magnetic field  $B$  of the third 30-degree dipole magnet, the magnetic rigidity ( $B\rho$ ) was accurately determined. The magnetic field  $B$  was deduced from the field mapping data and the actual current measurement applied by the power supply. The position of the centered beam including the scaling of the  $B$ -field for a selected charge state was determined with a precision of  $\pm 0.2$  mm. When the different targets were remotely inserted on the beam axis, the centering procedure at F3 was the same as was carried out without a target. The ion-optical dispersion from F2 to F3 was employed to take into account possible small deviations from the exact center at the TPC. The calibration of the ion-optical disper-



**Fig. 1.** Scheme of the experimental set up. The accelerated  $^{208}\text{Pb}$  ions, extracted at different energies from the SIS-18 synchrotron, are transported to and focused on a charge-changing foil placed at the entrance F0 of the FRS spectrometer. This foil has the function of providing a selected charge state, very close to the mean charge state, which the ions will populate during their interaction in the atomic-collision targets positioned at the F2 focal plane. The incident charge state is spatially selected at the F1 dispersive focal plane via application of horizontal slits. The energy-loss  $\Delta E$  and the resulting charge-state distribution  $f(q)$  are simultaneously measured at the focal plane F3 with a position-sensitive detector (TPC) installed at a distance of 54 m from the entrance of the FRS. A measured characteristic charge-state distribution is illustrated for a single field setting. The scale of the ion-optical plot is  $\pm 0.1$  m in the dispersive direction.

sion coefficient was especially easy in these experiments, because in each position spectrum at F3 several charge states were spatially dispersed and well separated. A characteristic example of the measured charge-state distribution is shown in Fig. 1.

For this experiment, (35, 50, 70, 100, and 280) MeV/u  $^{208}\text{Pb}^{67+}$  ions were slowly extracted from SIS-18 with intensities of the order of  $10^3$ – $10^4$  ions per spill. The spill duration was 10 s. This low intensity and long spill duration of the primary beam was chosen to avoid any significant radiation damage of the targets and rate effects of the particle detector performance.

The FRS was operated in a specially-tuned ion-optical mode to match the goals of the present experiment. The first requirement was that the beam spot size at F2 is smaller than the 5 mm apertures of the targets to avoid unwanted scattering. This condition must also hold for the 310 mm long gas cells with the same 5 mm aperture size at each side. We used two gas cells with different window thicknesses for the different ranges of the selected gas pressures. Practically, this means that the ion-optical dispersion ( $-3.7$  cm/%) and the corresponding magnification (0.56) were approximately halved compared to the standard FRS operation [21]. In addition, the size of the beam spot at F2 and the dispersion coefficient from F2 to F3 ( $-2.0$  cm/%) determine the possible ion-optical resolving power ( $\approx 900$ , for an overall spot size of 2 mm) for the energy-loss and charge-state distribution measurements. At the highest energies, these ion-optical parameters enable the measurements of the complete charge-state distribution with a single magnetic field setting. However, at the lower energies, different parts of the position spectra, obtained by scaling the magnetic fields, were merged. The efficiency and linearity of the TPC was measured and taken into account over the full acceptance range. The unambiguous charge-state identification was based on the magnetic field calibration and verified by the observable atomic shell-gap signature in the spectra.

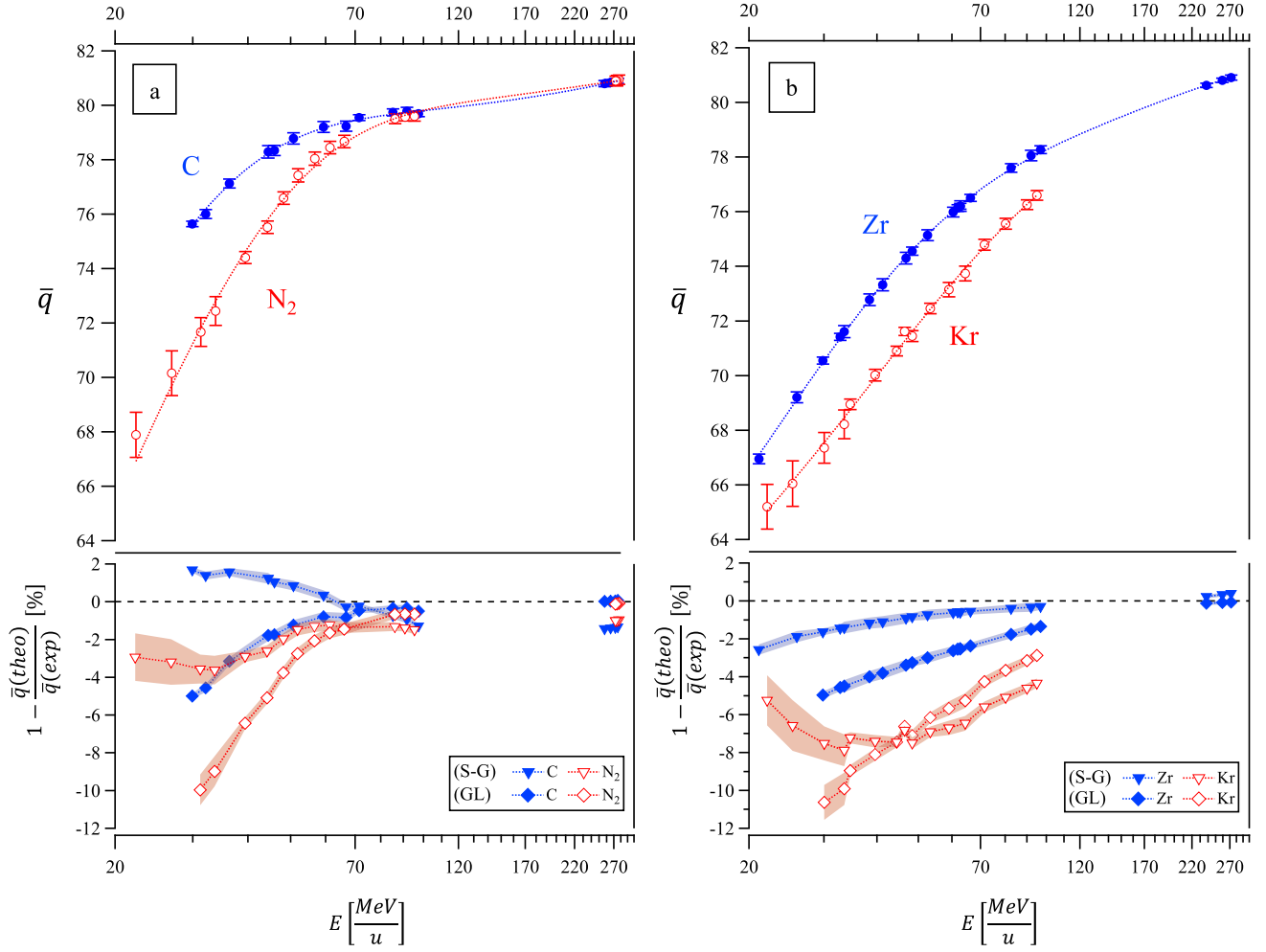
Exemplary results of our charge-state measurements are presented in Fig. 2 for lead ions emergent from different C,  $\text{N}_2$ , Kr, Zr targets at different energies. The data points were obtained at the different exit energies. In all cases, the targets were thick enough to provide equilibrium charge-state distributions. Possible influences of non-equilibrium were avoided by careful selection of the incident charge states of the projectiles, as explained above. At lower energies the measured mean charge states in solids (C, Zr)

are systematically higher than in the compared gases ( $\text{N}_2$ , Kr). The difference is approximately 5–6% at 30 MeV/u and has vanished by 280 MeV/u. The presented data of the gaseous targets were corrected for the influence of the gas-cell windows. This small correction was performed by extended GLOBAL [27] and MOCADI [28] computer simulations with adjustment of the charge-changing cross sections to the measurements of the separately measured pure window material.

A comparison of our measured results with theoretical predictions indicated deviations of up to 12%. We employed for this comparison the semi-empirical Schiwietz-Grande formula [26] and the predictions of the computer code GLOBAL [27]. Another important charge-state simulation code is ETACHA [29], which takes into account the temporary population of excited states during the passage of the target. Therefore ETACHA has in principle the potential to reproduce the gas-solid difference as observed in this experiment. However, in the recently improved ETACHA publication, it was restricted to ion-solid collisions [30]. Our charge-state measurements are presently used to extend and validate the computer code ETACHA.

The main conclusions from our charge-state measurements are: 1. The mean charge state of partially ionized Pb projectiles emerging from solids is higher than for gaseous targets. 2. The theoretical predictions for the mean charge states are not accurate enough to provide reliable stopping powers in the 1–2% domain and better. The deviations for charge states would result in approximately a factor two more deviations for the corresponding stopping-power values in this energy domain. 3. Guided by our results of the measured charge-state population, we can expect an observable Bohr-Lindhard density effect for stopping powers in the selected energy domain of this experiment.

The equilibrium charge-state distributions and the stopping powers were measured simultaneously for the same targets in the present experiment. For the energy-loss determination, the position distributions close to the TPC center were transformed on an event-by-event basis to the corresponding energy spectra. The measurements were always performed with and without a target inserted into the beam axis. In this way, the mean energy loss in different target thicknesses was determined with a typical accuracy of a few parts per thousand.



**Fig. 2.** Measured mean charge states ( $\bar{q}$ ) of  $^{208}\text{Pb}$  ions emergent with different energies from gaseous ( $\text{N}_2$ , Kr) and solid (C, Zr) targets. The number of  $\bar{q}$  data points is determined by both the number of selected accelerator energies and the number of targets with different thicknesses. The measured  $\bar{q}$  data are connected by a function approximation using a sum of two exponentials (dotted lines). The deviations of the experimental values from corresponding theoretical predictions are compared in the lower parts of the gas-solid pairs in a) and b). The experimental errors are illustrated by shadowed bands. The experimental values are compared with an empirical formula from Schiwietz and Grande (S-G) [26] and the widely-used computer program GLOBAL (GL) [27].

Besides the measurements of the mean energy loss  $\langle \Delta E \rangle$ , more parameters must be considered for accurate stopping-power experiments [31]. From this aspect, it is valuable to remember the basic definition:

$$\frac{dE}{dx} = \lim_{\Delta x \rightarrow 0} \frac{\langle \Delta E \rangle}{\Delta x}. \quad (1)$$

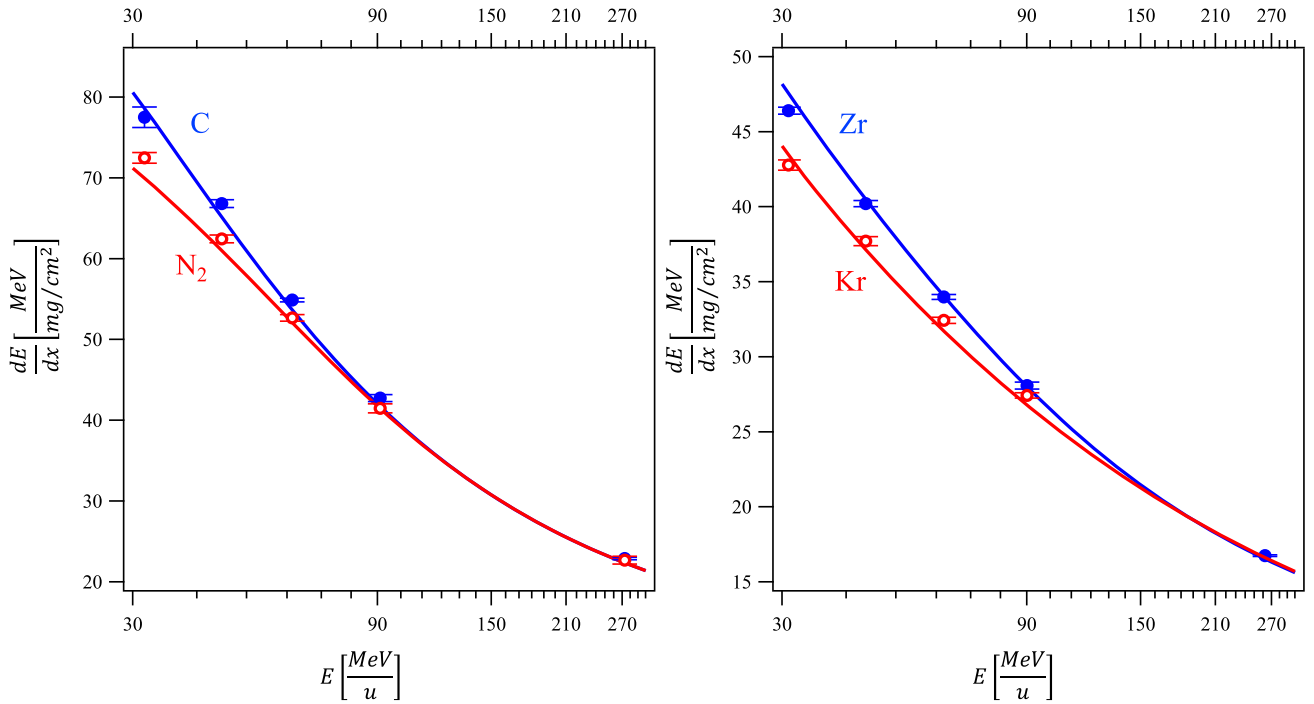
First of all, we have assured that in measurements of  $\langle \Delta E \rangle$  all impact-parameter events are accepted in the detector system, otherwise only restricted energy-loss measurements will be recorded. Furthermore, the targets should be thin and their thickness very well known, because the uncertainty of thickness contributes directly to the uncertainty of stopping power. The practical units of the thickness  $x$  and the stopping power  $dE/dx$  are  $\text{mg}/\text{cm}^2$  and  $\text{MeV}/(\text{mg}/\text{cm}^2)$ , respectively. There are several experimental methods applied in the literature to derive stopping-power values from different foil thicknesses [32,33]. We have used a method previously developed and applied by our group, where we have determined the experimental deviation from the corresponding theoretical prediction for different thicknesses of one target material. The energy dependence of the stopping power is theoretically well-known in the range of the present experiment. The procedure can be illustrated with the applied equation:

$$\Delta E(x) = \int_0^x \left( \frac{dE}{dx'} \right)_{\text{Theo.}} dx' + P(x), \quad (2)$$

where  $P(x)$  is the thickness-dependent difference after subtracting the theoretical energy loss from the experimental one. Performing a least-square fit for  $P(x)$  and taking both the uncertainties of the energy loss and thickness  $x$  into account, the experimental stopping power can be deduced by adding the  $dP/dx$  term to the theoretical stopping power:

$$\left( \frac{dE}{dx} \right)_{\text{Exp.}} = \left( \frac{dE}{dx} \right)_{\text{Theo.}} + \frac{dP}{dx}. \quad (3)$$

Note that due to this evaluation procedure, our experimental stopping power values can be given for any energy in the complete validity range of  $P(x)$ , thus the comparison of the gas-solid pairs could be presented in the figure at identical energies. The depicted five data points are selected at energies close to those corresponding to the mean thickness of the used targets. A function approximation using a sum of two exponentials of the mean-charge-state values allows to apply the  $\bar{q}$  values with a precision of better than  $10^{-3}$  for stopping power predictions in the measured energy range, see Fig. 2.



**Fig. 3.** Measured stopping powers of  $^{208}\text{Pb}$  ions in gases ( $\text{N}_2$ , Kr) and in solids (C, Zr) at different energies. Left panel: Measured stopping-power values in C foils (filled circles) and  $\text{N}_2$  gas (open circles). The solid lines are a comparison with the modified ATIMA program with the implementation of our measured  $\bar{q}$  values in the Lindhard-Sørensen theory. Right panel: Same presentation and comparison as in left panel but for the experimental values in Zr foils and Kr gas.

Our measured stopping-power values are presented in Fig. 3 for the same targets as discussed for our charge-state measurements above. The experimental data are represented by open and filled circles. The first observation is that the measured stopping powers in gases are systematically lower than the equivalent results in the solid targets of neighboring elements at the same velocity. The difference increases for lower energies up to (8–10)% and has vanished for the highest incident energy of 280 MeV/u.

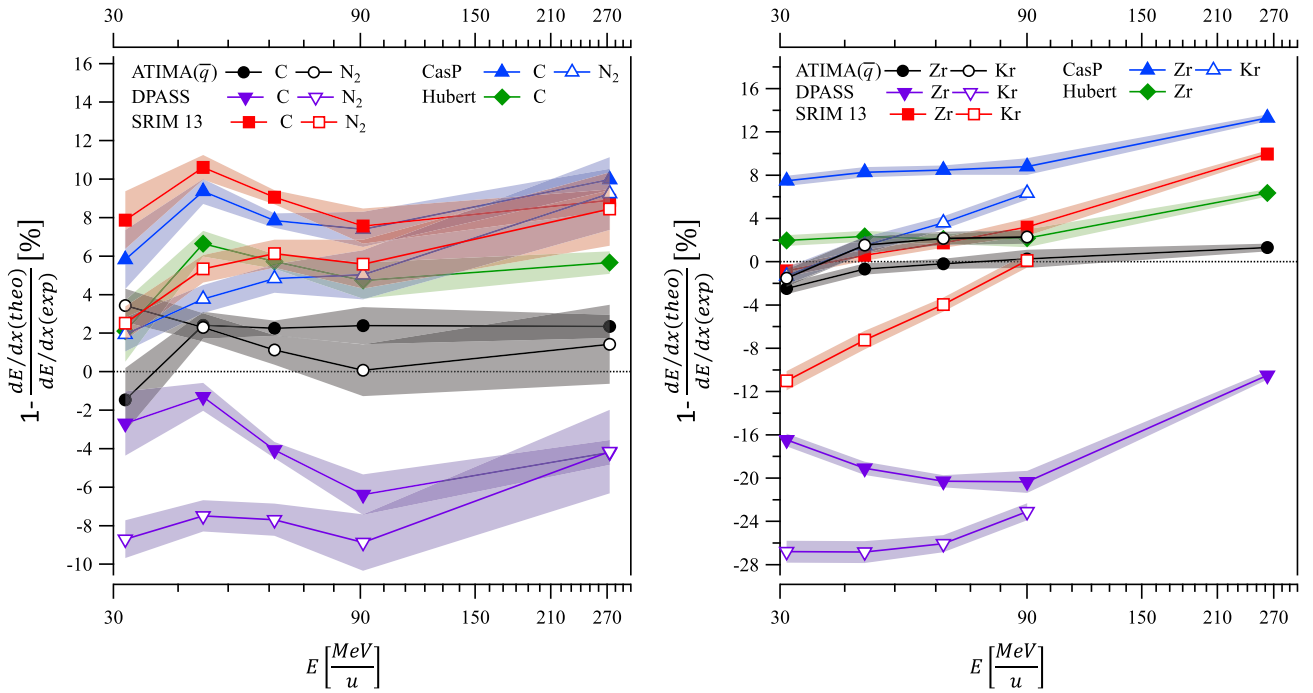
In Fig. 3, the solid lines represent the theoretical predictions by the ATIMA program [34] using the Lindhard-Sørensen theory [35] modified with the input of our measured mean charge states. For the additional correction terms including the Barkas term [36], we used also the experimental mean-charge values instead of the atomic number. The overall agreement with the data is better than 3% and confirms our discussion that accurate knowledge of the charge-state population is the key to theoretical improvements of stopping powers for partially-ionized projectiles in this velocity range. The latter statement is confirmed by strong disagreement when bare projectiles are assumed or semi-empirical formulas are applied. Comparisons with widely-used programs and tables (ATIMA [34], DPASS Version 2.00 [37,38], CasP Version 5.2 [39,40], Hubert-Tables [41], SRIM Version 2013 [42,43]) are shown in Fig. 4. The best agreement, as already mentioned above, is exhibited by ATIMA with the implementation of the measured mean charges of the present experiment, see Fig. 4. In case the mean charge of GLOBAL [27] is implemented in ATIMA the agreement is more than a factor 2 worse on average. Note that in the energy range of the present experiment, ATIMA applies the Lindhard-Sørensen (LS) theory [35] and can be modified optionally with  $\bar{q}$  taken either from the present experiment, from GLOBAL [27], or from the formulas of Ref. [26]. The widely-used SRIM program is based on a scaling of proton-stopping powers at the same velocity with an empirical effective charge. SRIM does not include density differences for gases and solids. The deviations from our results are up to 10%. The results from the Hubert tables are slightly better and show deviations of the order 5–7%. The Hubert Tables use also

the parameterization with an effective charge, derived from fits to experimental data in a relatively small velocity region, similar to the SRIM method, but scale the stopping power of alpha particles. Note that the Hubert Tables are only valid for solids. DPASS exhibits better agreement for the light elements, but deviates up to 27% for the heavier targets. The comparison with the CasP calculations shows better agreement with the gases and deviations up to 10% for solids.

In general, the widely-used slowing-down theories cannot accurately describe the present data, because the gas-solid difference is not included or the implementation of the charge-state population is inaccurate. One way to significantly improve the agreement between theory and experiment is demonstrated with our combination of the LS theory and implementation of the experimental data of the equilibrium mean charge states. With this goal in mind, we had measured also charge-changing cross sections of few-electron ions [44,45] to understand the different electron capture and loss processes under simplified conditions. The results of these experiments are implemented in computer codes, e.g., GLOBAL [46] and CHARGE [47]. However, the dependence of charge-changing cross sections on  $Z_1$ ,  $Z_2$  and the velocity  $v$  is complex and includes high powers, e.g., non-radiative electron capture  $\sigma_{cap} \propto Z_1^5 \times Z_2^5 \times v^{-11}$  [48]. Therefore, the limited number of cross-section measurements cannot directly contribute to improved stopping-power descriptions as the systematic equilibrium mean charge-state measurements do in the present experiment. The present excellent agreement with the implementation of the measured mean charge states also demonstrates that collisions with an impact parameter larger than the ionic radius of the projectile dominate the stopping power.

In summary, our stopping-power experiment clearly demonstrates: 1. The Bohr-Lindhard density effect for stopping powers is unambiguously verified in the energy range of the present experiment. 2. The charge states inside the solids are higher than those inside gases, in contradiction with the Betz-Grodzins model. 3. When the projectiles are nearly fully ionized the gas-solid differ-





**Fig. 4.** Left panel: The deviation of the experimental stopping powers of  $^{208}\text{Pb}$  ions in C foils and in  $\text{N}_2$  gas from the theoretical predictions of SRIM, DPASS, CasP, Hubert and ATIMA are presented. Note that the Hubert tables are published for solids only. Right panel: Same presentation and comparison as in the left panel but for the experimental values in Zr foils and Kr gas. The experimental errors are illustrated by colored bands.

ence vanishes. 4. The ATIMA stopping-power model, including the present measured mean charge-states and the Lindhard-Sørensen theory, results in an unprecedented accuracy of better than 3% in the studied energy region. The knowledge of the projectile charge-state distribution and the deviation from the Bethe theory are decisive factors to improve the accuracy of the theoretical predictions.

It is worth mentioning that the present experiment represents also a challenge in beam time and consists of more than 800 spectra due to the many field settings and parameters. The latter condition is in contrast to many other accelerator experiments where stopping data were obtained in short runs mainly during detector tests and nuclear physics measurements [9]. We can conclude that for future experiments, it is essential that stopping-power measurements for partially-ionized heavy ions are combined with simultaneous charge-state measurements with the same targets. Furthermore, the same efforts have to be made for energy-loss and target investigation as it was performed in the present experiment.

#### Declaration of competing interest

The authors declare that they have no known competing financial interests or personal relationships that could have appeared to influence the work reported in this paper.

#### Data availability

Data will be made available on request.

#### Acknowledgements

It is a great pleasure to acknowledge the excellent technical support of the engineers K.-H. Behr, T. Blatz, P. Schwarz and B. Szczepanczyk, the accelerator experts and the target laboratories at GSI and Technical University Darmstadt. We would like to thank Holger Brand for his extensive support and expertise in developing the LabVIEW interface for our experiment. We appreciate

important discussions with H. Albers on the impact of stopping power accuracy for nuclear spectrometer experiments. Furthermore, we thank P. Sigmund for fruitful discussions concerning this manuscript and valuable collaboration over more than 4 decades.

This work was supported by Justus-Liebig-Universität Gießen and GSI Helmholtzzentrum für Schwerionenforschung GmbH, Darmstadt under the JLU-GSI strategic Helmholtz partnership agreement.

This work was supported by the international project “PMW” of the Polish Minister of Science and Higher Education; active in the period 2022–2024; grant Nr 5237/GSIFAIR/2022/0.

The results presented here are based on the experiment S469, which was performed at the FRS at the GSI Helmholtzzentrum für Schwerionenforschung GmbH, Darmstadt (Germany) in the context of FAIR Phase-0.

Our special gratitude goes to J. Lindhard who inspired our atomic collision experiments at GSI over many years. Therefore, we would like to dedicate this publication to him as an outstanding teacher and friend.

#### References

- [1] R. Bimbot, S. Barbey, T. Benfoughal, F. Clavier, M. Mirea, N. Pauwels, S. Pierre, M. Rivet, G. Fares, A. Hachem, et al., Stopping powers of gases for very heavy ions, Nucl. Instrum. Methods Phys. Res., Sect. B, Beam Interact. Mater. Atoms 107 (1–4) (1996) 9–14, [https://doi.org/10.1016/0168-583X\(95\)00804-7](https://doi.org/10.1016/0168-583X(95)00804-7).
- [2] N. Bohr, The penetration of atomic particles through matter, Mat.-Fys. Medd. Danske Vid. Selsk. 18 (8) (1948) 1, <http://gymskiv.sdu.dk/MFM/kdvs/mfm%2010-19/mfm-18-8.pdf>.
- [3] P. Sigmund, Particle Penetration and Radiation Effects Volume 2, Springer Series in Solid-State Sciences, vol. 179, Springer, 2014.
- [4] J.J. Cowan, C. Sneden, J.E. Lawler, A. Aprahamian, M. Wiescher, K. Langanke, G. Martínez-Pinedo, F.-K. Thielemann, Origin of the heaviest elements: the rapid neutron-capture process, Rev. Mod. Phys. 93 (2021) 015002, <https://doi.org/10.1103/RevModPhys.93.015002>.
- [5] T. Ohnishi, T. Kubo, K. Kusaka, A. Yoshida, K. Yoshida, M. Ohtake, N. Fukuda, H. Takeda, D. Kameda, K. Tanaka, et al., Identification of 45 new neutron-rich isotopes produced by in-flight fission of a  $^{238}\text{U}$  beam at 345 MeV/nucleon, J. Phys. Soc. Jpn. 79 (7) (2010) 073201, <https://doi.org/10.1143/JPSJ.79.073201>.
- [6] J. Kurciewicz, F. Farion, H. Geissel, S. Pietri, C. Nociforo, A. Prochazka, H. Weick, J. Winfield, A. Estradé, P. Allegro, et al., Discovery and cross-section

- measurement of neutron-rich isotopes in the element range from neodymium to platinum with the frs, *Phys. Lett. B* 717 (4) (2012) 371–375, <https://doi.org/10.1016/j.physletb.2012.09.021>.
- [7] E. Blakely, C. Tobias, F. Ngo, S. Curtis, *Physical and radiobiological properties of heavy ions in relation to cancer therapy*, in: M. Pirruccello, C. Tobias (Eds.), *Biological and Medical Research with Heavy Ions at the BEVALAC, LBL 11220*, Berkeley UC Press, Berkeley, 1980, pp. 73–86.
  - [8] G. Kraft, Tumor therapy with heavy charged particles *Prog. Part. Nucl. Phys.* 45 (2000) S473–S544, [https://doi.org/10.1016/S0146-6410\(00\)00112-5](https://doi.org/10.1016/S0146-6410(00)00112-5).
  - [9] H. Geissel, H. Weick, C. Scheidenberger, R. Bimbot, D. Gardes, Experimental studies of heavy-ion slowing down in matter, *Nucl. Instrum. Methods Phys. Res., Sect. B, Beam Interact. Mater. Atoms* 195 (1–2) (2002) 3–54, [https://doi.org/10.1016/S0168-583X\(02\)01311-3](https://doi.org/10.1016/S0168-583X(02)01311-3).
  - [10] G. Savard, Large radio-frequency gas catchers and the production of radioactive nuclear beams, *J. Phys. Conf. Ser.* 312 (2011) 052004, <https://doi.org/10.1088/1742-6596/312/5/052004>.
  - [11] W.R. Plaß, T. Dickel, S. Purushothaman, P. Dendooven, H. Geissel, J. Ebert, E. Haettner, C. Jesch, M. Ranjan, M. Reiter, et al., The FRS ion catcher—a facility for high-precision experiments with stopped projectile and fission fragments, *Nucl. Instrum. Methods Phys. Res., Sect. B, Beam Interact. Mater. Atoms* 317 (2013) 457–462, <https://doi.org/10.1016/j.nimb.2013.07.063>.
  - [12] N.O. Lassen, Total charges of fission fragments in gaseous and solid media, *Phys. Rev.* 79 (6) (1950) 1016, <https://doi.org/10.1103/PhysRev.79.1016.2>.
  - [13] N. Bohr, J. Lindhard, Electron capture and loss by heavy ions penetrations through matter, *Mat.-Fys. Medd. Danske Vid. Selsk.* 28 (7) (1954) 1, <http://gymarkiv.sdu.dk/MFM/kdvs/mfm%2020-29/mfm-28-7.pdf>.
  - [14] H.D. Betz, L. Grodzins, Charge states and excitation of fast heavy ions passing through solids: a new model for the density effect, *Phys. Rev. Lett.* 25 (4) (1970) 211, <https://doi.org/10.1103/PhysRevLett.25.211>.
  - [15] Y. Laichter, N. Shafrir, Fine structure in the stopping powers and ranges of fission fragments in matter, *Nucl. Phys. A* 394 (1–2) (1983) 77–86, [https://doi.org/10.1016/0375-9474\(83\)90162-8](https://doi.org/10.1016/0375-9474(83)90162-8).
  - [16] R. Schramm, H.-D. Betz, Problems concerning the effective charge of Swift heavy ions traversing gaseous and solid targets, *Nucl. Instrum. Methods Phys. Res., Sect. B, Beam Interact. Mater. Atoms* 69 (1) (1992) 123–126, [https://doi.org/10.1016/0168-583X\(92\)95747-F](https://doi.org/10.1016/0168-583X(92)95747-F).
  - [17] H. Geissel, Y. Laichter, W. Schneider, P. Armbruster, Energy loss and energy loss straggling of fast heavy ions in matter, *Nucl. Instrum. Methods Phys. Res.* 194 (1–3) (1982) 21–29, [https://doi.org/10.1016/0029-554X\(82\)90483-9](https://doi.org/10.1016/0029-554X(82)90483-9).
  - [18] H. Geissel, Y. Laichter, W. Schneider, P. Armbruster, Observation of a gas-solid difference in the stopping powers of (1–10) MeV/u heavy ions, *Phys. Lett. A* 88 (1) (1982) 26–28, [https://doi.org/10.1016/0375-9601\(82\)90415-7](https://doi.org/10.1016/0375-9601(82)90415-7).
  - [19] R. Bimbot, C. Cabot, D. Gardes, H. Gauvin, I. Orliange, L. De Reilhac, K. Subotic, F. Hubert, Stopping power of gases for heavy ions: gas-solid effect: II. 2–6 MeV/u Cu, Kr and Ag projectiles, *Nucl. Instrum. Methods Phys. Res., Sect. B, Beam Interact. Mater. Atoms* 44 (1) (1989) 19–34, [https://doi.org/10.1016/0168-583X\(89\)90684-8](https://doi.org/10.1016/0168-583X(89)90684-8).
  - [20] D. Boehne, K. Blasche, B. Franczak, B. Franzke, H. Prange, R. Steiner, The performance of the SIS and developments at GSI, in: *Particle Accelerator*, vol. 1, 1990.
  - [21] H. Geissel, P. Armbruster, K.H. Behr, A. Brünle, K. Burkard, M. Chen, H. Folger, B. Franczak, H. Keller, O. Klepper, et al., The GSI projectile fragment separator (FRS): a versatile magnetic system for relativistic heavy ions, *Nucl. Instrum. Methods Phys. Res., Sect. B, Beam Interact. Mater. Atoms* 70 (1–4) (1992) 286–297, [https://doi.org/10.1016/0168-583X\(92\)95944-M](https://doi.org/10.1016/0168-583X(92)95944-M).
  - [22] C. Scheidenberger, H. Geissel, H. Mikkelsen, F. Nickel, T. Brohm, H. Folger, H. Irnich, A. Magel, M. Mohar, G. Münzenberg, et al., Direct observation of systematic deviations from the Bethe stopping theory for relativistic heavy ions, *Phys. Rev. Lett.* 73 (1) (1994) 50, <https://doi.org/10.1103/PhysRevLett.73.50>.
  - [23] C. Scheidenberger, H. Geissel, H. Mikkelsen, F. Nickel, S. Czajkowski, H. Folger, H. Irnich, G. Münzenberg, W. Schwab, T. Stöhlker, et al., Energy-loss-straggling experiments with relativistic heavy ions in solids, *Phys. Rev. Lett.* 77 (19) (1996) 3987, <https://doi.org/10.1103/PhysRevLett.77.3987>.
  - [24] H. Weick, H. Geissel, C. Scheidenberger, F. Attallah, D. Cortina, M. Hausmann, G. Münzenberg, T. Radon, H. Schatz, K. Schmidt, et al., Drastic enhancement of energy-loss straggling of relativistic heavy ions due to charge-state fluctuations, *Phys. Rev. Lett.* 85 (13) (2000) 2725, <https://doi.org/10.1103/PhysRevLett.85.2725>.
  - [25] H. Weick, H. Geissel, C. Scheidenberger, F. Attallah, T. Baumann, D. Cortina, M. Hausmann, B. Lommel, G. Münzenberg, N. Nankov, et al., Slowing down of relativistic few-electron heavy ions, *Nucl. Instrum. Methods Phys. Res., Sect. B, Beam Interact. Mater. Atoms* 164 (2000) 168–179, [https://doi.org/10.1016/S0168-583X\(99\)01025-3](https://doi.org/10.1016/S0168-583X(99)01025-3).
  - [26] G. Schiwietz, P. Grande, Improved charge-state formulas, *Nucl. Instrum. Methods Phys. Res., Sect. B, Beam Interact. Mater. Atoms* 175 (2001) 125–131, [https://doi.org/10.1016/S0168-583X\(00\)00583-8](https://doi.org/10.1016/S0168-583X(00)00583-8).
  - [27] C. Scheidenberger, T. Stöhlker, W. Meyerhof, H. Geissel, P. Mokler, B. Blank, Charge states of relativistic heavy ions in matter, *Nucl. Instrum. Methods Phys. Res., Sect. B, Beam Interact. Mater. Atoms* 142 (4) (1998) 441–462, [https://doi.org/10.1016/S0168-583X\(98\)00244-4](https://doi.org/10.1016/S0168-583X(98)00244-4).
  - [28] N. Iwasa, H. Geissel, G. Münzenberg, C. Scheidenberger, T. Schwab, H. Wollnik MOCADI, A universal Monte Carlo code for the transport of heavy ions through matter within ion-optical systems, *Nucl. Instrum. Methods Phys. Res., Sect. B, Beam Interact. Mater. Atoms* 126 (1–4) (1997) 284–289, [https://doi.org/10.1016/S0168-583X\(97\)01097-5](https://doi.org/10.1016/S0168-583X(97)01097-5).
  - [29] J. Rozet, A. Chetoui, P. Piquemal, D. Vernhet, K. Wohrer, C. Stephan, L. Tassan-Got, Charge-state distributions of few-electron ions deduced from atomic cross sections, *J. Phys., B At. Mol. Opt. Phys.* 22 (1) (1989) 33, <https://doi.org/10.1088/0953-4075/22/1/007>.
  - [30] E. Lamour, P.D. Fainstein, M. Galassi, C. Prigent, C. Ramirez, R.D. Rivarola, J.-P. Rozet, M. Trassinelli, D. Vernhet, Extension of charge-state-distribution calculations for ion-solid collisions towards low velocities and many-electron ions, *Phys. Rev. A* 92 (4) (2015) 042703, <https://doi.org/10.1103/PhysRevA.92.042703>.
  - [31] P. Sigmund, A. Schinner, Note on measuring electronic stopping of slow ions, *Nucl. Instrum. Methods Phys. Res., Sect. B, Beam Interact. Mater. Atoms* 410 (2017) 78–87, <https://doi.org/10.1016/j.nimb.2017.08.011>.
  - [32] P. Hvelplund, B. Fastrup, Stopping cross section in carbon of 0.2–1.5 MeV atoms with  $21 \leq Z_1 \leq 39$ , *Phys. Rev.* 165 (2) (1968) 408, <https://doi.org/10.1103/PhysRev.165.408>.
  - [33] R. Bimbot, S. Della Negra, D. Gardes, H. Gauvin, A. Fleury, F. Hubert, Stopping power measurements for 4–5 MeV/nucleon  $^{16}\text{O}$ ,  $^{40}\text{Ar}$ ,  $^{63}\text{Cu}$  and  $^{84}\text{Kr}$  in C, Al, Ni, Ag and Au, *Nucl. Instrum. Methods* 153 (1) (1978) 161–169, [https://doi.org/10.1016/0029-554X\(78\)90633-X](https://doi.org/10.1016/0029-554X(78)90633-X).
  - [34] H. Weick, et al., ATIMA program, <https://web-docs.gsi.de/~weick/atima/>, 1998.
  - [35] J. Lindhard, A.H. Sørensen, Relativistic theory of stopping for heavy ions, *Phys. Rev. A* 53 (4) (1996) 2443, <https://doi.org/10.1103/PhysRevA.53.2443>.
  - [36] J. Lindhard, The Barkas effect - or  $Z_1^3$ ,  $Z_1^2$ -corrections to stopping of Swift charged particles, *Nucl. Instrum. Methods* 132 (1976) 1–5, [https://doi.org/10.1016/0029-554X\(76\)90702-3](https://doi.org/10.1016/0029-554X(76)90702-3).
  - [37] A. Schinner, P. Sigmund, Expanded PASS stopping code, *Nucl. Instrum. Methods Phys. Res., Sect. B, Beam Interact. Mater. Atoms* 460 (2019) 19–26, <https://doi.org/10.1016/j.nimb.2018.10.047>.
  - [38] A. Schinner, P. Sigmund, DPASS program, <https://www.sdu.dk/en/dpass>, 2019.
  - [39] G. Schiwietz, P.L. Grande, Introducing electron capture into the unitary-convolution-approximation energy-loss theory at low velocities, *Phys. Rev. A* 84 (5) (2011) 052703, <https://doi.org/10.1103/PhysRevA.84.052703>.
  - [40] G. Schiwietz, P.L. Grande, CasP version 5.2, [https://www.helmholtz-berlin.de/people/gregor-schiwietz/casp\\_en.html](https://www.helmholtz-berlin.de/people/gregor-schiwietz/casp_en.html), 2014.
  - [41] F. Hubert, R. Bimbot, H. Gauvin, Range and stopping-power tables for 2.5–500 MeV/nucleon heavy ions in solids, *At. Data Nucl. Data Tables* 46 (1) (1990) 1–213, [https://doi.org/10.1016/0092-640X\(90\)90001-Z](https://doi.org/10.1016/0092-640X(90)90001-Z).
  - [42] J.F. Ziegler, M.D. Ziegler, J.P. Biersack, SRIM—the stopping and range of ions in matter (2010), *Nucl. Instrum. Methods Phys. Res., Sect. B, Beam Interact. Mater. Atoms* 268 (11–12) (2010) 1818–1823, <https://doi.org/10.1016/j.nimb.2010.02.091>.
  - [43] J. Ziegler, SRIM & TRIM, <http://www.srim.org/>, 2013.
  - [44] C. Scheidenberger, H. Geissel, T. Stöhlker, H. Folger, H. Irnich, C. Kozhuharov, A. Magel, P. Mokler, R. Moshhammer, G. Münzenberg, et al., Charge states and energy loss of relativistic heavy ions in matter, *Nucl. Instrum. Methods Phys. Res., Sect. B, Beam Interact. Mater. Atoms* 90 (1–4) (1994) 36–40, [https://doi.org/10.1016/0168-583X\(94\)95506-9](https://doi.org/10.1016/0168-583X(94)95506-9).
  - [45] H. Ogawa, H. Geissel, A. Fettohui, S. Fritzsche, M. Portillo, C. Scheidenberger, V. Shevelko, A. Surzhykov, H. Weick, F. Becker, et al., Gas-solid difference in charge-changing cross sections for bare and H-like nickel ions at 200 MeV/u, *Phys. Rev. A* 75 (2) (2007) 020703, <https://doi.org/10.1103/PhysRevA.75.020703>.
  - [46] C. Scheidenberger, H. Geissel, Penetration of relativistic heavy ions through matter, *Nucl. Instrum. Methods Phys. Res., Sect. B, Beam Interact. Mater. Atoms* 135 (1–4) (1998) 25–34, [https://doi.org/10.1016/S0168-583X\(97\)00639-3](https://doi.org/10.1016/S0168-583X(97)00639-3).
  - [47] T. Stöhlker, H. Geissel, H. Folger, C. Kozhuharov, P. Mokler, G. Münzenberg, D. Schardt, T. Schwab, M. Steiner, H. Stelzer, et al., Equilibrium charge state distributions for relativistic heavy ions, *Nucl. Instrum. Methods Phys. Res., Sect. B, Beam Interact. Mater. Atoms* 61 (4) (1991) 408–410, [https://doi.org/10.1016/0168-583X\(91\)95313-3](https://doi.org/10.1016/0168-583X(91)95313-3).
  - [48] I. Tolstikhina, M. Imai, N. Winckler, V. Shevelko, *Basic Atomic Interactions of Accelerated Heavy Ions in Matter*, Springer Series on Atomic, Optical, and Plasma Physics, Springer, 2018.